

### **Answer to a Reviewer 1:**

The authors thank the reviewer for the constructive comments on the paper. Our answers are given below:

1. We acknowledge that the theory described must be extended to account for the possible snow vertical inhomogeneity and possible finite thickness of a snowpack. These topics are out of scope of this paper. The abstract, introduction, and conclusions have been modified to account for your comment.
2. We also agree that the retrieval approach will not work well in case of polluted snow with the spectral absorption coefficients of pollutants, which do not follow the Angström law. The abstract, introduction, and conclusions have been modified to account for your comment. Of course, general equations (Eqs. 1-3) to solve the direct problem of snow optics presented in the paper can be used anyway. Eq. 1 has a misprint (R0 is missed before the exponential term). We have corrected this misprint in the final version.
3. All equations and definitions are explained in the text. We have also prepared the Appendix A with all definitions and units. Also we have prepared a special section (appendix B) on discussion of the retrieval errors as advised by you.
4. With respect to your comment related to the asymmetry parameter  $g$ , we confirm that this parameter depends on the shape of the grains. We have used the fixed value (0.75) in the determination of the grain size. Although the effective absorption length  $l$  (see Eq.14) can be derived from reflectance even if the value of  $g$  is not known. Therefore, we propose to use  $l$  for the characterization of natural snowpacks.
5. We have accounted for all your minor comments.

### **Answer to a Reviewer 2:**

The authors thank the reviewer for the constructive comments on the paper. Our answers are given below:

1. We have changed the sequence of the discussions of the measurements at different sites. Therefore, the numbering of figures has not been changed. The data shown in Figure 2 is related to Figure 1. So we prefer the sequence of figures as it stands.
2. Table 1 has been modified according your advices.

Line 42: We have mentioned in the conclusions that one can use just 1 wavelength to find the snow grain size in case of albedo measurements for clean snow. In case of reflectance measurements one needs to perform the measurements at two wavelengths (for clean snow).

Line 79: We have added an explanation related to Eq. 7 in the text.

Lines 84, 85, 108, 115, 174, 234, 242, 244,245-248, 267,276, 285-286, 293, 299-301, Figure 4: Done.

Lines 194, 204: We have prepared Appendix B to explain the derivations.

Lines 236-238: We had the measurements at 5 sites. Each measurement at each site has been performed 5 times and the average spectral curve has been found for all five sites. The text has been modified.

Lines 303-308: We agree that we do not retrieve refractive index of dust in this work. However, the extension of this work may lead to such retrievals. So we prefer to keep the text as it stands.

Line 319: We have modified the text taking into account your comment. Although we do not provide EAL in the Table. It can be calculated via the grain diameter as described in the paper.

Figure 3: The figure is clear and we do not think that the legend is really needed to clarify the discussion. Also we do not see a point in changing the scale.

All figures: We do not change the axis OX because different instruments operate in different spectral ranges.

# On the reflectance spectroscopy of snow

Alexander Kokhanovsky(1), Maxim Lamare(2,3), Biagio Di Mauro(4), Ghislain Picard  
(2), Laurent Arnaud (2), Marie Dumont (3), François Tuzet (3,2), Carsten Brockmann(5),  
Jason E. Box(6)

(1) VITROCISSET, Bratustrasse 7, D-64293 Darmstadt, Germany

(2) UGA, CNRS, Institut des Géosciences de l'Environnement (IGE), UMR 5001,  
Grenoble, 38041, France

(3) Meteo-France–CNRS, CNRM UMR 3589, Centre d'Etudes de la Neige, Grenoble,  
France

(4) Department of Earth and Environmental Sciences, University of Milano-Bicocca, Piazza  
della Scienza, 1 20126 Milan, Italy

(5) Brockmann Consult, Max Planck Strasse 2, Geesthacht, Germany

(6) Geological Survey of Denmark and Greenland (GEUS), Copenhagen, Denmark

## Abstract

We propose a system of analytical equations to retrieve snow grain size and absorption coefficient of pollutants from snow reflectance or snow albedo measurements in the visible and near-infrared regions of the electromagnetic spectrum, where snow single scattering albedo is close to 1.0. It is assumed that ice grains and impurities (e.g., dust, black and brown carbon) are externally mixed, the snow layer is semi-infinite and vertically and horizontally homogeneous. The influence of close-packing effects on reflected light intensity are assumed to be small and ignored. The system of nonlinear equations is solved analytically in the assumption that impurities have the spectral absorption coefficient, which obey the Angström power law, and the impurities influence the registered spectra only in the visible and not at near-infrared (and vice versa for ice grains). The theory is validated using spectral reflectance measurements and albedo of clean and polluted snow at various locations (Antarctica Dome C, European Alps). The technique to derive the snow albedo (plane and spherical) from

29 reflectance measurements at a fixed observation geometry is proposed. The technique also  
30 enables the simulation of hyperspectral snow reflectance measurements in the broad spectral  
31 range from ultraviolet to the near-infrared for a given snow surface in the case, if the actual  
32 measurements are performed at restricted number of wavelengths (2-4, depending on the type  
33 of snow and the measurement system).  
34

35

## 36 **1. Introduction**

37 The reflective properties of clean and polluted snow are of importance for various applications  
38 including climate (Hansen and Nazarenko, 2007) and environmental pollution (Nazarenko et al.,  
39 2017) studies. The spectral snow reflectance is usually studied in the framework of the radiative  
40 transfer theory. The application of the numerical methods for the solution of the radiative  
41 transfer equation for snow layers has been performed by Mishchenko et al. (1999), Stamnes et al.  
42 (2011), and He et al. (2018) among others. The approximate solutions of the radiative transfer  
43 equation useful for snow optics and spectroscopy applications have been developed by Warren  
44 and Wiscombe (1980), Wiscombe and Warren (1980) and Kokhanovsky and Zege (2004). In this  
45 work, we propose an analytical snow albedo and reflectance model, which can be used to derive  
46 near - surface snow optical and microphysical properties using measurements at just two to four  
47 wavelengths in the visible and near-infrared depending on the measurement system and type of  
48 snow. In particular, we present the method for the determination of snow grain size, absorption  
49 Angström coefficient and spectral absorption coefficient of impurities embedded in the snow  
50 matrix assuming an external mixture of snow grains and impurities. A technique to derive the  
51 snow albedo from reflectance measurements is also presented. The absorption and extinction of  
52 light by snow grains is treated in the framework of a geometrical optical approximation. The  
53 absorption coefficient of impurities is modeled using the Angström power law. All derivations

54 are performed in the framework of the asymptotic radiative transfer theory (see, e.g.,  
55 Kokhanovsky and Zege, 2004, Zege et al., 2011). It is assumed that the snow layer is vertically  
56 and horizontally homogeneous and semi-infinite. Therefore, the effects of the finite layer  
57 thickness are ignored.

58

## 59 **2. Theory**

### 60 **2.1 The snow reflectance**

61 The snow reflectance  $R$  (equal to unity for ideal white Lambertian reflectors, see Appendix A)  
62 can be presented in the following way using approximate asymptotic radiative transfer theory  
63 (Kokhanovsky and Zege, 2004):

$$64 \quad R = R_0 r_s^x, \quad (1)$$

65 where  $x = u(\mu_0)u(\mu) / R_0$ ,  $R_0$  is the reflectance of a semi-infinite non-absorbing snow layer,

$$66 \quad u(\mu_0) = \frac{3}{7}(1 + 2\mu_0), \quad \mu_0 \text{ is the cosine of the solar zenith angle, } \mu \text{ is the cosine of the viewing}$$

67 zenith angle,  $r_s$  is the snow spherical albedo:

$$68 \quad r_s = e^{-y}, \quad (2)$$

69 where

$$70 \quad y = 4 \sqrt{\frac{1 - \omega_0}{3(1 - g)}}, \quad (3)$$

71  $g$  is the asymmetry parameter,  $\omega_0$  is the single scattering albedo. Let us introduce the probability  
 72 of photon absorption  $\beta \equiv 1 - \omega_0$ . It is equal as the ratio of absorption  $\kappa_{abs}$  and extinction  $\kappa_{ext}$   
 73 coefficients:

$$74 \quad \beta = \frac{\kappa_{abs}}{\kappa_{ext}}, \quad (4)$$

75 where

$$76 \quad \kappa_{abs} = \kappa_{abs}^{ice} + \kappa_{abs}^{pol}. \quad (5)$$

77 The first and second terms in Eq. (5) correspond to the ice grains and pollutants, respectively.  
 78 We assume that scattering and extinction of light by impurities is much smaller than that by ice  
 79 grains and, therefore (Kokhanovsky and Zege, 2004),

$$80 \quad \kappa_{ext} = \frac{3c}{d}. \quad (6)$$

81 Here,  $d = 1.5\bar{V} / \bar{S}$  is the effective diameter of ice grains,  $\bar{V}$  is the average volume of grains,  $\bar{S}$   
 82 is their average projected area averaged over all directions (equal to  $\Sigma/4$  for convex particles in  
 83 random orientation, where  $\Sigma$  is the average surface area and  $c$  is the volumetric concentration of  
 84 the snow grains). The value of  $c$  is equal to the volume of grains in unit volume of snow  
 85 ( $c = N\bar{V}$ , where  $N$  is the number of snow grains in unit volume of snow ( $\text{cm}^{-3}$ )). It is related to  
 86 the dry snow density  $\rho_s$  by the following relation:  $\rho_s = c\rho_i$ , where  $\rho_i$  is the bulk ice density.

87 The product of the effective diameter  $d$  and the bulk ice absorption coefficient  $\alpha$  is a small  
 88 number in the visible and near-infrared. Then it follows (Kokhanovsky and Zege, 2004, see their  
 89 Eq. (37) for the absorption path length inversely proportional to the absorption coefficient) that:

$$90 \quad \kappa_{abs}^{ice} = B\alpha c, \quad (7)$$

91 where  $B$  is the grain shape-dependent parameter (absorption enhancement parameter),  
 92  $\alpha = \frac{4\pi\chi}{\lambda}$ , where  $\chi$  is the imaginary part of the ice refractive index at the wavelength  $\lambda$ .

93 We present the absorption coefficient of pollutants in snow as

$$94 \quad \kappa_{abs}^{pol}(\lambda) = \kappa_0 \lambda^{-m}, \quad (8)$$

95 where  $\kappa_0 \equiv \kappa_{abs}^{pol}(\lambda_0)$ ,  $\lambda_0 = 1 \mu m$ ,  $m$  is the absorption Angstrom coefficient.

96 It follows from Eqs. (4)-(8):

$$97 \quad \beta = \frac{B\alpha d}{3} + \beta^{pol}, \quad (9)$$

98 where

$$99 \quad \beta^{pol} = \frac{\kappa_0 \lambda_0^{-m} d}{3c} \quad (10)$$

100 and therefore:

$$101 \quad y = \frac{4}{3} \sqrt{\frac{(B\alpha + \kappa_0 \lambda_0^{-m} c^{-1})d}{1-g}}. \quad (11)$$

102 Let the parameter  $z = y^2$ , from which it follows that:

103 
$$z = (\alpha + f \mathcal{R}^{\sigma^n})l, \quad (12)$$

104 where

105 
$$f = \frac{\kappa_0^*}{B}, \quad (13)$$

106  $\kappa_0^* = \kappa_0 / c$  and

107 
$$l = \xi d \quad (14)$$

108 is the effective absorption length (EAL) and

109 
$$\xi = \frac{16B}{9(1-g)} \quad (15)$$

110 is a grain shape (but not the grain size) dependent parameter.

111 The parameter  $l$  can be determined directly from reflectance or albedo measurements, enabling  
112 also the determination of the grain diameter  $d = l / \xi$  assuming a particular shape of grains. It has  
113 been found that the asymmetry parameter of crystalline clouds is usually in the range 0.74-0.76  
114 in the visible (Garret, 2008). The asymmetry parameter  $g$  for snow has not been measured so far  
115 *in situ* but we shall assume that it is close to that in crystalline clouds and adopt the value 0.75. It  
116 follows from experimental studies of Libois et al. (2014) that  $B=1.6$  on average. Therefore, it  
117 follows (see Eq. 15):  $\xi \approx 11.38$ .

118 Using the EAL, the equations for the snow reflectance and spherical albedo may be simplified.

119 Namely, it follows:

120 
$$R = R_0 \exp(-x\sqrt{(\alpha + f \mathcal{R}^{\sigma^n})l}), \quad (16)$$

121 
$$r_s = \exp(-\sqrt{(\alpha + f \mathcal{R}^{\sigma^n})l}). \quad (17)$$

122 The plane albedo can be derived as well (Kokhanovsky and Zege, 2004):



123 
$$r = \exp(-u(\mu_0))\sqrt{(\alpha + f\lambda^{\rho/\sigma^m})l}. \quad (18)$$

124 The relationship between the albedo and the reflectance  $R$  is given in Appendix A. It follows  
 125 from Eq. (16) that the spectral reflectance of polluted snow is determined by four *a priori*  
 126 unknown parameters:  $l, R_0, f, m$ . They can be estimated from the measurements of reflectance at  
 127 four wavelengths. This also enables the determination of the spectral reflectance (and albedo, see  
 128 Eq.(18)) at the visible and near – infrared wavelengths at an arbitrary  $\lambda$ . It follows:

129 
$$R_1 = R_0 \exp(-x\sqrt{(\alpha_1 + f\lambda_1^{\rho/\sigma^m})l}), \quad (19)$$

130 
$$R_2 = R_0 \exp(-x\sqrt{(\alpha_2 + f\lambda_2^{\rho/\sigma^m})l}) \quad (20)$$

131 
$$R_3 = R_0 \exp(-x\sqrt{(\alpha_3 + f\lambda_3^{\rho/\sigma^m})l}) \quad (21)$$

132 
$$R_4 = R_0 \exp(-x\sqrt{(\alpha_4 + f\lambda_4^{\rho/\sigma^m})l}) \quad (22)$$

133 where the numbers 1, 2, 3, and 4 signify the wavelengths used. Equations (19)-(22) can be used  
 134 to compute four unknown parameters given above, and, therefore, determine reflectance and  
 135 albedo at any wavelength in the visible and the near-infrared using Eqs. (16)-(18). Let us assume  
 136 that the spectral channels are selected in a way that the effects of ice absorption can be neglected  
 137 in the first two channels ( $\lambda_1, \lambda_2$ ) and effects of absorption by pollutants are negligible in the  
 138 second pair of channels ( $\lambda_3, \lambda_4$ ). This situation is typical of not heavily polluted snow. Then it  
 139 follows instead of Eqs. (19)-(22):

140 
$$R_1 = R_0 \exp(-x\sqrt{f\lambda_1^{\rho/\sigma^m}l}), \quad (23)$$

141 
$$R_2 = R_0 \exp(-x\sqrt{f\lambda_2^0/m}l), \quad (24)$$

142 
$$R_3 = R_0 \exp(-x\sqrt{\alpha_3}l), \quad (25)$$

143 
$$R_4 = R_0 \exp(-x\sqrt{\alpha_4}l). \quad (26)$$

144 Eqs. (25), (26) can be used to find the pair  $(l, R_0)$ :

145 
$$R_0 = R_3^{\varepsilon_1} R_4^{\varepsilon_2}, \quad l = \frac{1}{x^2 \alpha_4} \ln^2 \left[ \frac{R_4}{R_0} \right], \quad (27)$$

146 where  $\varepsilon_1 = 1/(1-b)$ ,  $\varepsilon_2 = 1/(1-b^{-1})$ ,  $b = \sqrt{\alpha_3/\alpha_4}$ . Then it follows from Eqs. (23), (24) that:

147 
$$m = \frac{\ln(p_1/p_2)}{\ln(\lambda_2/\lambda_1)}, \quad (28)$$

148 
$$f = \frac{p_1 \lambda_1^0}{x^2 l}, \quad (29)$$

149 where  $p_k = \ln^2(R_k/R_0)$ . In case of the absence of pollutants, Eqs. (27) remain valid. However,

150 the parameters  $m$  and  $f$  are undefined and  $R = R_0 \exp(-x\sqrt{\alpha}l)$ .

151 One may also derive the impurity absorption coefficient at the wavelength

152  $\lambda_0$  normalized to the concentration of ice grains  $c$  (see Eq. (13)):

153 
$$\kappa_0^* = Af, \quad (30)$$

154 where  $f$  is given by Eq.(29). The normalized absorption coefficient at each wavelength can also  
 155 be found using Eqs. (8), (28), (30).

156 To determine the concentration of pollutants ( $c_p$ ) one must either know in advance or determine  
 157 the impurity volumetric absorption coefficient defined as:

$$158 \quad K(\lambda_0) = \frac{\bar{C}_{abs}(\lambda_0)}{\bar{V}}, \quad (31)$$

159 where  $\bar{C}_{abs}$  is the average absorption cross section of impurities and  $\bar{V}$  is the average volume of absorbing  
 160 impurities. Namely, it follows by definition:

$$161 \quad c_p = \frac{\kappa_0}{K(\lambda_0)} \quad (32)$$

162 and

$$163 \quad \mathcal{E} = \frac{\kappa_0^*}{K(\lambda_0)}, \quad (33)$$

164 where  $\mathcal{E} = c_p / c$ .

165 The value of  $K(\lambda_0)$  can be found, if one knows the type of pollutants and their microphysical properties.  
 166 In particular, it follows for the impurities much smaller than the wavelength  $\lambda_0$  (van de Hulst, 1981) that :

$$167 \quad K(\lambda_0) = F\alpha_{pol}(\lambda_0), \quad (34)$$

168 where

$$169 \quad \alpha_{pol}(\lambda_0) = \frac{4\pi\chi_{pol}(\lambda_0)}{\lambda_0} \quad (35)$$

170 is the pollutant bulk absorption coefficient,  $\chi_{pol}(\lambda_0)$  is the imaginary part of pollutant refractive  
 171 index and  $n_{pol}$  is the real part of the pollutant refractive index,

$$172 \quad F = \frac{9n_{pol}}{(n_{pol}^2 + 1 - \chi_{pol}^2)^2 + 4n_{pol}^2 \chi_{pol}^2} . \quad (36)$$

173 It follows that  $F = 0.9$  for soot (assuming that  $n=1.75$ ,  $\chi_{pol} = 0.47$  in the visible). One can see  
 174 that  $\mathcal{E}$  can be found if one knows the refractive index of absorbing Rayleigh particles in  
 175 advance.

176 In particular, it follows for soot impurities that:

$$177 \quad \mathcal{E} = \frac{Ap_1 \lambda_1^{9/6}}{x^2 l F \alpha_{pol}(\lambda_0)} . \quad (37)$$

178 In case of non-Rayleigh scatterers, one needs to know not only the refractive index but  
 179 also the particle size distribution and shape of particles, enabling the determination of the  
 180 impurity volumetric absorption coefficient  $K(\lambda_0)$  and, therefore, the normalized concentration  
 181 of impurities

$$182 \quad \mathcal{E} = \frac{Ap_1 \lambda_1^{9/6}}{x^2 l K(\lambda_0)} . \quad (38)$$

183

184

185

## 2.2. The snow albedo

### 186 2.2.1 Theory

187 If the plane albedo is the measured physical quantity one needs to find only three constants:

188  $l, f, m$ .

189 The respective analytical equations can be presented as:

$$190 \quad r_1 = \exp(-u(\mu_0)\sqrt{(\alpha_1 + f\lambda_1^m)l}), \quad (39)$$

$$191 \quad r_2 = \exp(-u(\mu_0)\sqrt{(\alpha_2 + f\lambda_2^m)l}), \quad (40)$$

$$192 \quad r_3 = \exp(-u(\mu_0)\sqrt{(\alpha_3 + f\lambda_3^m)l}). \quad (41)$$

193 We shall assume that the last channel is not influenced by impurities and the first two channels  
194 are not influenced by the absorption of light by grains. Then it follows that:

$$195 \quad r_1 = \exp(-u(\mu_0)\sqrt{f\lambda_1^m l}), \quad (42)$$

$$196 \quad r_2 = \exp(-u(\mu_0)\sqrt{f\lambda_2^m l}), \quad (43)$$

$$197 \quad r_3 = \exp(-u(\mu_0)\sqrt{\alpha_3 l}). \quad (44)$$

198 The EAL can be found from Eq. (44):

$$199 \quad l = \frac{\ln^2 r_3}{u^2(\mu_0)\alpha_3}. \quad (45)$$

200 It follows from Eqs. (42), (43) that:

$$201 \quad m = \frac{\ln(\psi_2 / \psi_1)}{\ln(\lambda_1 / \lambda_2)}, f = \frac{\psi_1 \lambda_1^{9/8}}{u^2(\mu_0)l}, \quad (46)$$

202 where  $\psi_k = \ln^2 r_k$ .

203 In case of unpolluted snow, one derives:

$$204 \quad r = \exp(-u(\mu_0)\sqrt{\alpha l}). \quad (47)$$

205 Eq. (45) can be used to find the effective absorption length and, therefore, the spectral albedo of  
206 unpolluted snow at any wavelength using Eq. (47). If not plane but rather spherical albedo is  
207 measured, then all equations presented in this section are valid except one should assume that  
208  $u = 1$  and substitute  $r$  by  $r_s$  (Kokhanovsky and Zege, 2004).

### 209 3. Experiment

#### 210 3.1 The measurements of the plane albedo

211 We have applied the technique developed above to the measured spectral plane albedo both for  
212 polluted and pure snow. Therefore, in-situ spectral albedo measurements were obtained from two  
213 different field sites located in the French Alps (polluted snow) and in Antarctica (clean snow).

214 The spectral albedo of a spring alpine snowpack was measured at the Col du Lautaret field site  
215 (45°2' N, 6°2' E, 2100 m a.s.l.) in the French Alps. The measurements were performed using a  
216 non-automated version of the spectrometer system described above. The hand-held instrument  
217 has a single light collector, located at the end of 3 m boom placed 1.5 m above the surface. The  
218 boom is rotated by the operator to successively acquire the downward and upward solar

219 radiation. The spectral albedo data (each spectral albedo measurement at a given point is an  
220 average of five measurements) at several locations close to the location Col du Lautaret field site  
221 was obtained on 12th April, 2017 across a 100 m transect, in attempt to account for spatial  
222 variability. The measurements were acquired in clear sky conditions, with a solar zenith angle  
223 varying between  $47.9^\circ$  and  $52.2^\circ$ .

224 The results of comparison of measurements and the theory presented above are illustrated in  
225 Fig.1 at the Col du Lautaret field site. The parameters  $l, f, m$  have been found from Eqs. (42)-  
226 (44) and the measurements at the wavelengths  $\lambda_1 = 400nm, \lambda_2 = 560nm, \lambda_3 = 1020nm$ . At other  
227 measurement sites across a transect the results of the inter-comparison are excellent and similar  
228 to that presented in Fig.1. Therefore, the theory can be used to derive snow optical and  
229 microphysical properties even for polluted snowpack. The derived spectral probability of photon  
230 absorption for the case shown in Fig. 1 is presented in Fig.2. The derived absorption coefficient  
231 (assuming  $c=1/3$ ), the grain diameter  $d$  and the absorption Angström parameter  $m$  for five sites  
232 across the transect are listed in Table 1 (lines 1-5). It follows that the value of  $m$  is in the range  
233 2.4 - 4.1 consistent with the identified presence of dust particles in snow (Doherty et al., 2010).  
234 The pure black carbon impurities have the values of  $m$  close to one. The grain diameter is in the  
235 range 1.7-2.2 mm consistent with low values of snow albedo at 1020nm (see Fig.1). Wiscombe  
236 and Warren (1981) have calculated the dependence of the clean snow spectral albedo at the solar  
237 zenith angle 60 degrees and several grain radii and presented it in their Fig.8. It follows from  
238 their calculations that the albedo decreases from 0.8 to 0.4 while the diameter of grains changes  
239 from 0.1 to 2mm. It follows from our Fig.1 that the measured plane albedo is close to 0.45  
240 signifying the dominance of large grains in the snowpack as reported in Table 1.

241 The spectral albedo of pure snow (very low amount of impurities) was measured at Dome C  
242 (75°5' S, 123°17' E), in Antarctica using an automated spectral radiometer (Libois et al., 2015;  
243 Picard et al., 2016; Dumont et al., 2017). The instrument is composed of two individual heads  
244 located approximately 1.5 m above the surface. Each head contains two cosine receptors facing  
245 upward and downward, which receive the incident solar radiation and the reflected radiation. The  
246 collectors are connected to a MAYA2000 PRO Ocean Optics spectrometer with fibre optics  
247 through an optical switch. Radiation is measured over 350-2500 nm spectral range with an  
248 effective spectral resolution of 3 nm. Albedo was calculated as the ratio of the upward and  
249 downward spectral irradiance. The full description of the instrument and the processing steps to  
250 calculate the spectral albedo are given by Picard et al. (2016). The spectral albedo measurements  
251 used here were made on the 10<sup>th</sup> January 2017, with a solar zenith angle of 63.2°, during clear  
252 sky conditions assessed by ground observations.

253 The results of the application of the proposed technique to the pure snow (no pollution) albedo  
254 measured in Antarctica are illustrated in Fig.3. Application of our technique results in excellent  
255 agreement with measured albedo over pure snow (now pollution) in Antarctica. Because the  
256 snow at Dome C is clean/pristine, the value of  $f$  is negligible, resulting in snow albedo depending  
257 only on the effective absorption length/grain size, which has been derived at a single wavelength  
258 (1020nm). The derived grain diameter for the case presented in Fig.3 is equal to 0.5mm. The  
259 retrieval error estimation is presented in Appendix B.

260

261

262



263  
264  
265  
266  
267  
268  
269  
270  
271  
272  
273  
274  
275  
276  
277  
278  
279  
280  
281  
282  
283  
284

### 3.2 The measurements of the spectral reflectance

The application of the developed theory to the measurements of the spectral reflectance is presented in Fig.4 for two locations with different dust loads (39.6ppm and 107.4ppm). The spectral reflectance of snow was measured in the European Alps (Artavaggio plains, 1650m a.s.l., 45°55'56.70"N; 9°31'33.28" E) at the solar zenith angle equal to 52 degrees. The measurements were made on March 14<sup>th</sup> 2014, after a major transport and deposition of mineral dust from the Saharan desert. The event was very intense, and it was reported in the recent scientific literature regarding snow optical properties, (Di Mauro et al., 2015; Dumont et al., 2017), atmospheric chemistry and physics (Belosi et al., 2017), and also microbiology (Weil et al., 2017). The dust transport event deposited fine mineral dust particles from the atmosphere via wet deposition, according to the BSC-DREAM-8b model (Basart et al., 2012). Spectral measurements of snow were made using a field spectrometer (Field Spec Pro, Analytical Spectral Devices, ASD). This instrument features a spectral range of 350-2500 nm, a full width at half maximum of 5–10 nm, and a spectral resolution of 1 nm. Data presented here were collected under clear sky conditions at noon. Incident radiation was estimated using a Lambertian Spectralon panel. Reflected radiance was divided by incident radiance, and the hemispherical conical reflectance factor was calculated for two plots containing 39.6 and 107.4 ppm of dust. Dust concentration was measured with a Coulter Counter by integrating particles with a diameter smaller than 18  $\mu\text{m}$ . Spectral measurements were performed at nadir using a bare optical fiber (field of view of 25°) at 80 cm from the snow sample. Both the optical fiber and the spectralon panel were equipped with an optical level. Further details on this dataset can be found in Di Mauro et al. (2015).

285 One can see that the theory works well not only for the albedo measurements (see the  
 286 previous section) but also for the reflectance measurements for polluted snow layers. In  
 287 particular, our results are closer to the measurements as compared to the theoretical model  
 288 described by Flanner et al. (2007) (see Fig.4b in Di Mauro et al., 2015). The derived parameters  
 289 are given in Table 1 (lines 6-7). The value of  $m$  is  $4.1$  for the case with the  $39.6\text{ppm}$  dust  
 290 concentration and it is  $6.4$  for the case with  $107.4$  dust concentration. Because the difference is  
 291 quite large for the close locations we conclude that snow also contained other pollutants (say,  
 292 soot) and the determined value of  $m$  represents the combined effect with larger values of  $m$  for  
 293 larger concentrations of dust, which is consistent with other observations of this parameter in  
 294 snow (Doherty et al., 2010). The retrieved absorption coefficient of snow pollutants (at the  
 295 wavelength  $\lambda^* = 560\text{nm}$ ) is  $0.1191\text{ m}^{-1}$  for the dust concentration  $39.6\text{ppm}$  and it is  $0.3123\text{ m}^{-1}$   
 296 for the dust concentration of  $107.4\text{ ppm}$ . Assuming that the dust chemical composition and also  
 297 the dust particle size distribution are the same at both locations we can assume that the ratio of  
 298 absorption coefficients at two locations should be equal to the ratio of dust concentrations. The  
 299 difference between the two ratios is  $<3\%$ , which is within the measurement uncertainty ( $10\%$  for  
 300 dust load measurements), and suggesting that the retrieved absorption coefficients at the two  
 301 sites are consistent with each other.

302 The mass absorption coefficient (MAC) can be estimated using:

$$303 \quad K_m = \frac{\kappa_{abs}^{pol}(\lambda^*)}{\mathcal{E}\rho c}, \quad (48)$$

304 where  $\rho$  is the density of the substance of impurities. Assuming that:

$$305 \quad \rho = 2.62\text{ g/cm}^3 \text{ (as for quartz)}, \quad c = 1/3, \quad \mathcal{E} = 107.4\text{ ppm} \text{ and } \kappa_{abs}^{pol}(\lambda^*) = 0.3123\text{ m}^{-1}, \quad (49)$$

306 one can derive that:

$$307 \quad K_m = 0.0033m^2 / g, \quad (50)$$

308 which is consistent with the values of MAC given by Utry et al.(2015) (e.g.,  
309  $0.0023m^2 / g$  for quartz and  $0.0051m^2 / g$  for illite (see their Table 1)).

#### 310 **4. Conclusions**

311 In this work, we have presented a sequence of analytical equations, which can be used to  
312 determine the snow grain size, the absorption coefficient of impurities, and the absorption  
313 Angström coefficient of surface snow impurities from the snow reflectance measured at four  
314 wavelengths: two in the visible and two in the near infrared as suggested by Warren (2013). In  
315 the case of albedo measurements just three wavelengths can be used to find main snow  
316 properties. For unpolluted snow, it is enough to perform the measurements at two wavelengths  
317 (for reflectance measurements) or just at a single wavelength (for albedo measurements) in the  
318 near-infrared to determine the snow grain size.

319 In principle, the refractive index of dust and dust size distribution can be also determined using  
320 derived spectral absorption coefficient of dust and assuming the shape of dust particles.  
321 However, we did not make an attempt for such retrievals in this work. The method for the  
322 retrieval of the complex refractive index and single scattering optical properties of dust deposited  
323 in mountain snow based on exact radiative transfer calculations has been proposed by McKenzie  
324 Siles et al. (2016) in the assumption that local optical properties of dust grains can be simulated  
325 assuming the spherical shape of particles. Their method is based on the extraction of dust grains  
326 from snowpack. Our technique does not require such a complicated procedure.

327 We have demonstrated how snow albedo can be derived from spectral reflectance measurements  
328 avoiding complicated integration with respect to the observation geometry (azimuth, viewing  
329 angle). The last point is useful for the determination of the snow *albedo* from spectral *reflectance*  
330 measurements (say, from aircraft or satellite) at a fixed observation geometry. Although the  
331 comprehensive validation of the retrievals has not been attempted, we have found that the ratio  
332 of derived absorption coefficients of pollutants at two concentrations is close to the ratio of  
333 pollutant concentrations derived independently, which indeed should be the case taking the  
334 proximity of two measurement sites with different dust loads. The general validity of the  
335 approach is proven using field measurements (Alps, Antarctica) of both spectral reflectance and  
336 plane albedo.

337 The determination of the EAL  $l$  (unlike the effective grain diameter  $d$ ) both from reflectance  
338 and albedo measurements is practically insensitive to *a priori* unknown shape of ice crystals.  
339 Therefore, this length may be useful for the characterization of snowpack microstructure (in  
340 addition to the grain size  $d$ ). The results presented in this work are useful for the interpretation of  
341 snow properties using both reflectance spectroscopy (Hapke, 2005) and imaging spectrometry  
342 (Dozier et al., 2009). It is assumed that the semi - infinite snow layer is vertically and  
343 horizontally homogeneous. The effects of the snow layer finite thickness, close packing effects,  
344 snow vertical inhomogeneity, possible internal mixture of pollutants in snow grains, and  
345 underlying surface albedo (ice, soil, grass) are ignored.

346  
347  
348

## 350 Appendix A. Nomenclature

Physical parameter	Notation	Units	Definition	Comments
Snow absorption coefficient	$\kappa_{abs}$	$m^{-1}$	$N\bar{C}_{abs}$	$N$ -number of snow grains in unit volume( $m^{-3}$ ) $\bar{C}_{abs}$ -average absorption cross section of grains ( $m^2$ )
Snow extinction coefficient	$\kappa_{ext}$	$m^{-1}$	$N\bar{C}_{ext}$	$N$ -number of snow grains in unit volume( $m^{-3}$ ) $\bar{C}_{ext}$ -average extinction cross section of grains ( $m^2$ )
Probability of photon absorption	$\beta$	-	$\kappa_{abs} / \kappa_{ext}$	$\beta \ll 1$ in the approximation studied
Snow single scattering albedo	$\omega_0$	-	$1 - \beta$	close to 1 in the approximation studied
Snow asymmetry parameter	$g$	-	$g = \frac{1}{2} \int_0^\pi p(\theta) \sin \theta \cos \theta d\theta$	$\frac{1}{2} \int_0^\pi p(\theta) \sin \theta d\theta = 1$ $\theta$ is the scattering angle(equal to $\pi$ in the exact backward scattering direction) $p(\theta)$ is the conditional probability of photon scattering in a given direction specified by the angle $\theta$ (phase function)
Bulk ice absorption coefficient	$\alpha$	$m^{-1}$	$\frac{4\pi\chi(\lambda)}{\lambda}$	$\chi(\lambda)$ - imaginary part of bulk ice refractive index $\lambda$ - wavelength
Volumetric absorption coefficient of pollutants	$K$	$m^{-1}$	$\bar{C}_{abs}^{pol} / \bar{V}_p$	$\bar{C}_{abs}^{pol}$ -average absorption cross section of impurities in snow ( $m^2$ ), $\bar{V}_p$ is their average volume( $m^3$ ), $K$ is <i>proportional</i> to the bulk absorption coefficient of impurities in case they are much larger as compared to

				the wavelength (and weakly absorbing) or much smaller as compared to the wavelength (so called Rayleigh scatterers). The coefficient of proportionality (absorption enhancement factor) depends on the shape of particles and real part of their complex refractive index.
Effective absorption length	$l$	$m^{-1}$	$\frac{\ln^2 r_s}{\alpha}$ (for clean dry snow)	$r_s = \exp(-\sqrt{\alpha}l)$ $r_s$ - spherical albedo $\alpha$ - bulk ice absorption coefficient This definition holds for clean dry snow only The general definition for dry snow is given by Eq. (17)
Reflectance	$R(\mu_0, \mu, \varphi)$	-	$I^\uparrow(\mu_0, \mu, \varphi) / I_{Lamb}^\uparrow(\mu_0)$	Ratio of intensity of light reflected from a given snowpack to that of an ideal Lambertian surface with albedo 1.0 $(\mu_0, \mu, \varphi)$ - cosine of the solar zenith angle, cosine of viewing zenith angle, and relative azimuth, respectively
Plane albedo	$r(\mu_0)$	-	$2 \int_0^1 \bar{R}(\mu_0, \mu, \varphi) \mu d\mu$	$\bar{R} = \frac{1}{2\pi} \int_0^\pi R(\mu_0, \mu, \varphi) \varphi d\varphi$ - reflectance averaged with respect to the azimuth, black sky albedo
Spherical albedo	$r_s$	-	$2 \int_0^1 r(\mu_0) \mu_0 d\mu_0$	white sky albedo
Volumetric concentration of grains	$c$	-	$N\bar{V}$	$N$ - number concentration of grains, $\bar{V}$ - average volume of grains, $c$ - fraction of unit volume occupied by ice grains (usually around 0.3)
Mass concentration of	$\rho_s$	$gm^{-3}$	$N\bar{m}$	$N$ - number concentration of grains,

grains (snow density)				$\bar{m} = \rho_i \bar{V}$ - average mass of grains, $\rho_i$ - bulk ice density, $\rho_s = \rho_i c$ (for dry snow)
Bulk ice density	$\rho_i$	$gm^{-3}$	-	$\rho_i = 916.7 kg / m^3$ at $0^\circ C$
Bulk pollutant density	$\rho_p$	$gm^{-3}$	-	
Volumetric concentration of impurities	$c_p$	-	$N_p \bar{V}_p$	$N_p$ - number concentration of pollution particles, $\bar{V}_p$ - average volume of pollution particles, $c$ - fraction of unit volume occupied by impurities
Normalized volumetric concentration of impurities	$\epsilon$	-	$c_p / c$	$\epsilon = \frac{\rho_i}{\rho_s} c_p$ $\rho_i$ - bulk ice density, $\rho_s$ - snow density, $c_p$ - volumetric concentration of impurities
Effective diameter of grains	$d$	$m$	$\frac{3\bar{V}}{2\bar{S}}$	equal to the diameter for the collection of spherical grains of the same size, $\bar{V}$ - average volume of grains, $\bar{S}$ - average cross section of grains (perpendicular to incident light beam),

351

352

353

354

355

356

357

358 **Appendix B. The retrieval error estimation**

359 **1. The effective absorption length and diameter of grains**

360 Let us consider the error budget for the retrieved snow parameters. To simplify, we assume that  
361 the snow parameters are derived using albedo measurements.

362 The value of  $l$  is determined from measurements just at a single wavelength in the framework of  
363 the theory given above. It follows from Eq. (45):

364 
$$\frac{\Delta l}{l} = K \frac{\Delta r_3}{r_3}, \quad (\text{B.1})$$

365 where

366 
$$K = \frac{2}{\ln r_3}. \quad (\text{B.2})$$

367 Therefore, the relative effective absorption length retrieval error is directly proportional to the  
368 relative measurement error in the measured albedo. Larger values of  $l$  correspond to the smaller  
369 albedo. So one conclude that that the error of retrieval of larger values of EAL are generally  
370 smaller (see Eq.(B.2)). For the cases, presented in Figs. 1 and 2, the wavelength 1020nm has  
371 been used in the retrieval process and one finds that  $K$  is equal to -2.5 and -5.8, respectively.  
372 Assuming the measurement error of 3%, one derives that EAL is determined with the accuracy -  
373 7.5 and -17.4 %, respectively with better accuracy for the observations in Alps, because the  
374 albedo is lower there. Also we see that the overestimation of the albedo in the experiment leads  
375 to the underestimation of the EAL and other way around in case measurements which  
376 underestimate the snow albedo because  $K$  is negative. Because  $K$  generally decreases with the



377 wavelength one must use the largest wavelengths to have better accuracy (say, 1020nm instead  
378 of 865nm). The wavelength should not be above 1200nm or so (depending on the snow grain  
379 size) because the underlying theory valid for weakly absorbing media only. So strong ice  
380 absorption bands must be avoided. The value of the snow grain size is proportional to the value  
381 of  $l$ . Therefore, our conclusions are also valid for the derived snow grain size assuming that one  
382 knows the parameter  $\xi$  ( see Eq.15) exactly. However, this parameter is known with some error.

383 The uncertainty in the parameter  $\xi = 16B/3(1-g)$  is difficult to access because we rely on a priori  
384 value for the snow asymmetry parameter and the absorption enhancement parameter  $B$ . We use  
385 the following values:  $B=1.6$ ,  $g=0.75$ . The reported values of  $g$  for for crystalline clouds do not  
386 go above 0.8. Therefore, the module of the absolute error in the parameter  $1-g$  is smaller than  
387 0.05 (and the relative error is below 20%). The value of  $B$  is usually in the range: 1.4-1.8 and,  
388 therefore, the absolute error in the parameter  $B$  is equal approximately to  $\pm 0.2$  and, therefore,  
389 the relative error is  $\pm 12.5\%$ . It follows that the absolute value of the maximal relative error in  
390 the parameter  $\xi$  is close to 24%. The error could be smaller in case the assumptions used in the  
391 derivations are closer to the actual snow conditions. We find that the maximal relative error in  
392 the derived grain diameter for the cases shown in Fig. 1, 2 is 25-30% depending on the snow  
393 type, which is substantially larger as compared to the error in the estimation of EAL.

394

395

396

397

398 **2. The spectral absorption coefficient of pollutants**

399 Let us consider the error budget for the retrieved spectral absorption coefficient of  
 400 pollutants. The absolute error of the retrieved parameter  $\Delta x$  is defined as

401 
$$\Delta x = \sqrt{\sum_{j=1}^J \left[ \frac{\partial x}{\partial y_j} \right]^2 \Delta y_j^2} . \quad (\text{B.3})$$

402 This error depends on  $j$  measurement errors of reflectance/albedo at  $j$ -channel  $\Delta y_j$ , where  $J$  is  
 403 the number of channels used to retrieve the corresponding parameter assuming that there are no  
 404 forward model errors. It is a difficult task to estimate the forward model error theoretically. It  
 405 depends on the specific type of snowpack.

406 It follows from Eqs. (46), (B.3) :

407 
$$\frac{\Delta f}{f} = \sqrt{\Upsilon_1^2 \left[ \frac{dr_1}{r_1} \right]^2 + \Upsilon_3^2 \left[ \frac{dr_3}{r_3} \right]^2}, \quad \frac{\Delta m}{m} = \sqrt{\Pi_1^2 \left[ \frac{dr_1}{r_1} \right]^2 + \Pi_2^2 \left[ \frac{dr_2}{r_2} \right]^2}, \quad (\text{B.4})$$

408 where

409 
$$\Upsilon_n = \frac{2}{\ln r_n}, \quad \Pi_n = \frac{2}{\ln r_n \ln(\psi_2 / \psi_1)}. \quad (\text{B.5})$$

410 We conclude that the errors of the pair  $(f, m)$  determination increase, if the selected wavelengths  
 411 at two channels in the visible are too close and if the logarithm of albedo at selected channels is  
 412 close to unity (say, weak concentration of pollutants for the channels in the visible). The albedo  
 413 decreases for the cases with illumination closer to nadir. Therefore, to reduce errors one needs to  
 414 use the measurements with larger deviations of Sun from the horizon direction.

415

The absorption coefficient of pollutants is given by the following equation ( see Eqs. (8), (13),(30)):

416

417

$$\kappa_{abs}^{pol} = Bcf \lambda^m. \tag{B.6}$$

418

Therefore, one derives

419

$$\frac{\Delta \kappa_{abs}^{pol}}{\kappa_{abs}^{pol}} = \sqrt{\left[\frac{\Delta B}{B}\right]^2 + \left[\frac{\Delta f}{f}\right]^2 + \left[\frac{\Delta c}{c}\right]^2 + \ln^2(\lambda) \left[\frac{\Delta m}{m}\right]^2}. \tag{B.7}$$

420

One concludes that the errors in the estimated snow volumetric concentration  $c$  (snow density, see Appendix A), the absorption enhancement coefficient  $B$ , and also pair  $(f,m)$  must be combined to estimate the total error in the retrieved spectral absorption coefficient of impurities in snow. The errors are lower, if one is interested in the spectral absorption coefficient of impurities normalized to its value at a specific wavelength defined as

421

422

423

424

425

$$R_{abs}^{pol} \equiv \frac{R_{abs}^{pol}(\lambda)}{R_{abs}^{pol}(\lambda_w)}, \tag{B.8}$$

426

where  $\lambda_w$  is the selected wavelength (say, 550nm).

427

One derives for this coefficient:

428

$$R_{abs}^{pol}(\lambda) \equiv \left(\frac{\lambda}{\lambda_w}\right)^{-m} \tag{B.9}$$

429 and, therefore, only the accuracy of the determination of absorption Angstroem exponent  
430 influences the result:

$$431 \quad \frac{\Delta \kappa_{abs}^{pol}}{\kappa_{abs}^{pol}} = \ln(\lambda / \lambda_0)^{-m} \frac{\Delta m}{m}. \quad (B.10)$$

432 An important point is the determination of concentration of pollutants in snow from optical  
433 remote sensing data. In principle the concentration of pollutants can be found, if the absorption  
434 coefficient of pollutants at a given wavelength is known. For instance, it follows by definition  
435 (see Eq. (31) for the definition of the volumetric absorption coefficient of impurities  $K$ ):

$$436 \quad c_p = \frac{\kappa_{abs}^{pol}(\lambda)}{K(\lambda)}.$$

437 Therefore, uncertainty in the derived or assumed value of  $K$  (or mass extinction coefficient  
438  $K_m = K / \rho_p$ , where  $\rho_p$  is the density of the substance of a pollutant) influences the retrieval error  
439 in addition to uncertainty of the derived absorption coefficient of pollutants  $\kappa_{abs}^{pol}(\lambda)$ . One can see  
440 that the determination of the concentration of pollutants from optical remote sensing of  
441 snowpack is a very challenging task.

442 In particular, one finds that the positive bias in the measured albedo in the visible will lead to  
443 the underestimation of the concentration of pollutants (assuming that the grain size is exactly  
444 known). It should be pointed out that in most cases the concentration of pollutants is so small  
445 that it can not be assessed using optical instruments (change in reflectance is inside experimental

446 measurement error). This issue has been discussed by Zege et al. (2011) and Warren (2013).

447 Similar conclusions hold also if the reflectance (and not albedo) is the measured quantity.

448

## 449 **5. Acknowledgments**

450 This work was mainly supported by the European Space Agency in the framework of ESRIN

451 contract No. 4000118926/16/I-NB “Scientific Exploitation of Operational Missions (SEOM)

452 Sentinel-3 Snow (Sentinel-3 for Science, Land Study 1: Snow)”. CNRM/CEN and IGE are part of

453 labex OSUG@2020. Measurements in the French Alps were funded by the ANRJJCJ grant EBONI

454 16-CE01-0006 and at Dome C by ANR JCJC MONISNOW 1-JS56-005-01.

455

456 **References**

457 S. Basart, S., C. Pérez, S. Nickovic, E. Cuevas, and J. M. Baldasano, "Development and  
458 evaluation of the BSC-DREAM8b dust regional model over Northern Africa, the Mediterranean  
459 and the Middle East", *Tellus B*, vol. 64, 2012, doi:10.3402/tellusb.v64i0.18539, 2012.

460 F. Belosi, M. Rinaldi, S. Decesari, L. Tarozzi, A. Nicosia, A., and G. Santachiara, "Ground  
461 level ice nuclei particle measurements including Saharan dust events at a Po Valley rural site  
462 (San Pietro Capofiume, Italy)", *Atmospheric Research*, vol. 186, pp. 116–126,  
463 <https://doi.org/10.1016/J.ATMOSRES.2016.11.012>, 2017.

464 B. Di Mauro, F. Fava, L. Ferrero, R. Garzonio, G. Baccolo, B. Delmonte, and R. Colombo,  
465 "Mineral dust impact on snow radiative properties in the European Alps combining ground,  
466 UAV, and satellite observations", *J. Geophys. Res. Atmos.*, vol. 120, pp. 6080–6097,  
467 doi:10.1002/2015JD023287, 2015.

468 S. J. Doherty, S. G. Warren, T. C. Grenfell, A. D. Clarke, and R. E. Brandt, "Light-absorbing  
469 impurities in Arctic snow", *Atmos. Chem. Phys.*, vol. 10, 11647–11680, 2010.

470 J. Dozier, R. O. Green, A. W. Nolin, and T. H. Painter, "Interpretation of snow properties from  
471 imaging spectrometry", *Remote Sens. Env.*, vol. 113, pp. S25–S37, 2009.

472 M. Dumont, L. Arnaud, G. Picard, Q. Libois, Y. Lejeune, P. Nabat, and S. Morin, S. "In situ  
473 continuous visible and near-infrared spectroscopy of an alpine snowpack". *The Cryosphere*,  
474 vol. 11, N3, pp. 1091–1110, <https://doi.org/10.5194/tc-11-1091-2017>, 2017.

475 M. G. Flanner, C. S. Zender, J. T. Randerson, and P. J. Rash, "Present – day climate forcing and  
476 response from black carbon in snow", *J. Geophys. Res Atmos.*, vol.112, D11202, doi:  
477 10.1029/2006JD008003, 2007.

478 T. J. Garrett, "Observational quantification of the optical properties of cirrus cloud", *Light*  
479 *Scattering Reviews* (ed. by A. Kokhanovsky), 3, 1-26, Praxis-Springer, 2008.

480 J. Hansen, and L. Nazarenko, 2004: "Soot climate forcing via snow and ice albedos", *Proc.*  
481 *Natl. Acad. Sci.*, 101, 423-428, doi:10.1073/pnas.2237157100, 2004.

482 B. Hapke, *Theory of reflectance and emittance spectroscopy*, Cambridge: Cambridge University  
483 Press, 2005.

484 C. He, K.-N. Liou, Y. Takano, P. Yang, L. Qi, and F. Chen, "Impact of grain shape and multiple  
485 black carbon internal mixing on snow albedo: parameterization and radiative effect analysis", *J.*  
486 *Geophys. Res.*, 123, 1253-1268, 2018.

487 A. A. Kokhanovsky, E.P. Zege, "Scattering optics of snow", *Appl. Optics*, vol. 43, N7, pp.1589-  
488 1602, 2004.

489 Q. Libois, G. Picard, M. Dumont, L. Arnaud, C. Sergent, E. Pougatch, M. Sudul, and D. Vial, "  
490 Experimental determination of the absorption enhancement parameter of snow", *J. Glaciology*,  
491 60, N 222, 2014.

492 Q. Libois, G. Picard, L. Arnaud, M. Dumont, M. Lafaysse, S. Morin, and E.  
493 Lefebvre, "Summertime Evolution of Snow Specific Surface Area close to the Surface on the  
494 Antarctic Plateau," *The Cryosphere*, 9, N6, 2383-2398, 2015.

495 S. McKenzie Skiles, T. Painter, G. S. Okin, "A method to retrieve the spectral complex refractive

496 index and single scattering optical properties of dust deposited in mountain snow’’, J.  
497 *Glaciology*, 63, N237, 133-147.

498 M. I. Mishchenko, J.M. Dlugach, E.G. Yanovitskij, and N.T. Zakharova, ’’Bidirectional  
499 reflectance of flat, optically thick particulate layers: An efficient radiative transfer solution and  
500 applications to snow and soil surfaces’’, *J. Quant. Spectrosc. Radiat. Transfer*, vol. 63, pp. 409-  
501 432, doi:10.1016/S0022-4073(99)00028-X, 1999.

502 Y. Nazarenko, S. Fournier, U. Kurien, R. B. Rangel-Alvarado, O. Nepotchatykh, P. Seers, P. A.  
503 Ariya, ’’Role of snow in the fate of gaseous and particulate exhaust pollutants from gasoline-  
504 powered vehicles’’. *Environmental Pollution*, 223, 665 DOI: 10.1016/j.envpol.2017.01.082,  
505 2017

506 G. Picard, Q. Libois, L. Arnaud, G. Verin, and M. Dumont, ’’Development and calibration of an  
507 automatic spectral albedometer to estimate near-surface snow SSA time series.’’ *The  
508 Cryosphere*, 10, N3, 1297-1316, 2016.

509 K. Stamnes, B. Hamre, J. J. Stamnes, G. Ryzikov, C. Biryulina, R. Mahoney, B. Haus, and A.  
510 Sei, ’’Modeling of radiation transport in coupled atmosphere-snow-ice-ocean systems’’, *J.  
511 Quant. Spectrosc. Radiat. Transfer*, 112, 714-726, 2011.

512 N. Utry, T. Ajtai, M. Pinter, E. Tombacz, E. Illes, Z. Bozoki, and G. Szabo, ’’Mass-specific  
513 optical absorption coefficients and imaginary part of the complex refractive indices of mineral  
514 dust components measured by a multi-wavelength photoacoustic spectrometer’’, *Atmos. Meas.  
515 Techniques*, 8, 401-410, 2015.

516 H. C. Van de Hulst, *Light scattering by small particles*, N.Y: Dover, 1981.



517 S. G. Warren, W. J. Wiscombe, "A model for spectral albedo of snow: II. Snow containig  
518 atmospheric aerosols", *J. Atmos. Sci.*, vol. 37, pp. 2734-2745, 1980.

519 S. G. Warren, "Can black carbon in snow be detected by remote sensing", *J. Geophys. Res.*,  
520 *Atmospheres*, 118, 779-786, 2013.

521 T. Weil, C. De Filippo, D. Albanese, C. Donati, M. Pindo, L. Pavarini, and F. Miglietta, "Legal  
522 immigrants: invasion of alien microbial communities during winter occurring desert dust  
523 storms", *Microbiome*, vol. 5, No 1, <https://doi.org/10.1186/s40168-017-0249-7>, 2017.

524 W. J. Wiscombe, and S. G. Warren, "A model for spectral albedo of snow: I. Pure snow", *J.*  
525 *Atmos. Sci.*, vol. 37, pp. 2712-2733.

526 E. P. Zege, I. L. Katsev, A. V. Malinka, A. S. Prikhach, G. Heygster, and H. Wiebe, "Algorithm  
527 for retrieval of the effective snow grain size and pollutants amount from satellite  
528 measurements", *Rem. Sens. Env.*, 115, 2674-2685.

529

530

531 Tables

532

533 Table 1. The derived snow parameters for the five samples. The value of  $c$  is assumed to be equal

534  $1/3$ , which leads to the extinction length ( $l_{ext} = 1/\kappa_{ext}$ ) to be equal to the effective grain diameter

535  $d$ . The absorption coefficient is given at the wavelengths  $\lambda_0=1000\text{nm}$  and  $\lambda^* = 560\text{nm}$ .

536	N	$\kappa_{abs}^{pol}(\lambda_0), m^{-1}$	$\kappa_{abs}^{pol}(\lambda^*), m^{-1}$	$m$	$d, mm$	Site
537	1	0.0182	0.1954	4.1	2.1	Col du Lautaret (site 1)
538	2	0.0342	0.2668	3.5	2.2	Col du Lautaret (site2)
539	3	0.1073	0.7194	3.3	1.7	Col du Lautaret (site 3)
540	4	0.0769	0.5324	3.3	1.9	Col du Lautaret (site 4)
541	5	0.0943	0.3848	2.4	2.2	Col du Lautaret (site 5)
542	6	0.0111	0.1191	4.1	2.5	Artavaggio plains (site 1)
543	7	0.0077	0.3123	6.4	1.5	Artavaggio plains (site 2)

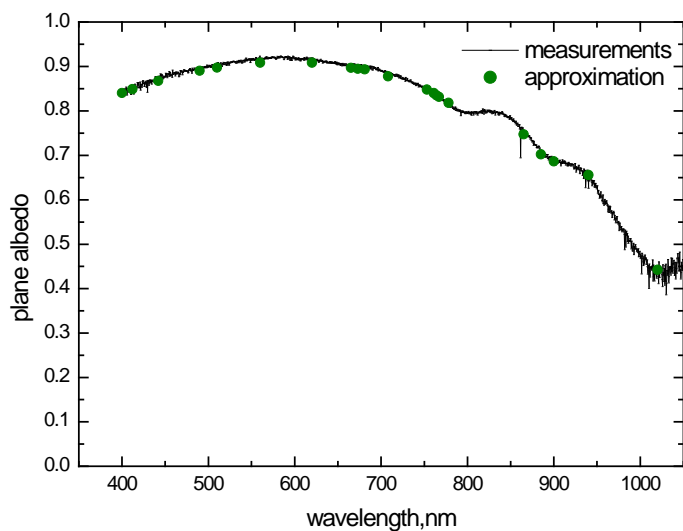
544

545

546

547

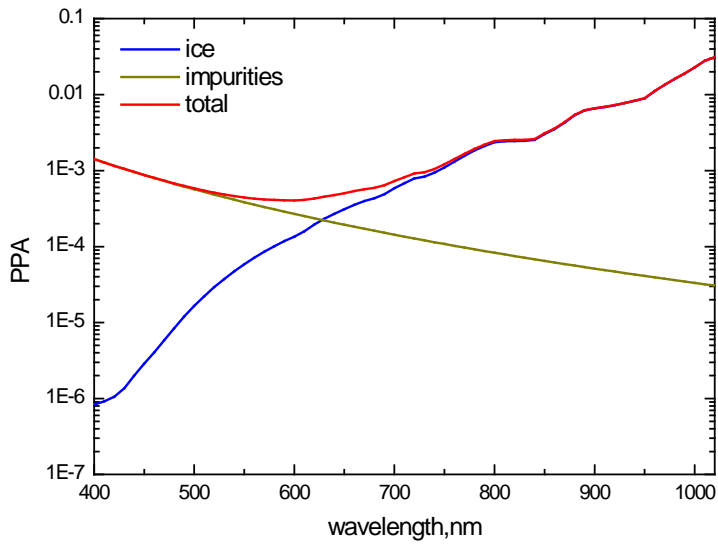
548 Figures



549

550 Fig.1. The intercomparison of theory (symbols) with experimental measurements of plane albedo  
551 (line, no noise removed) performed in French Alps (45°2' N, 6°2' E, 2100 m a.s.l.) obtained on  
552 12/04/2017. The plane albedo is an average of 5 measurements performed between 08h55 and  
553 09h30 UTC for a polluted (by dust) snowpack. The solar zenith angle for the measurements was  
554 between 47° and 49°. The noise of measurements has not been removed and clearly seen in the  
555 near infrared portion of the spectrum.

556

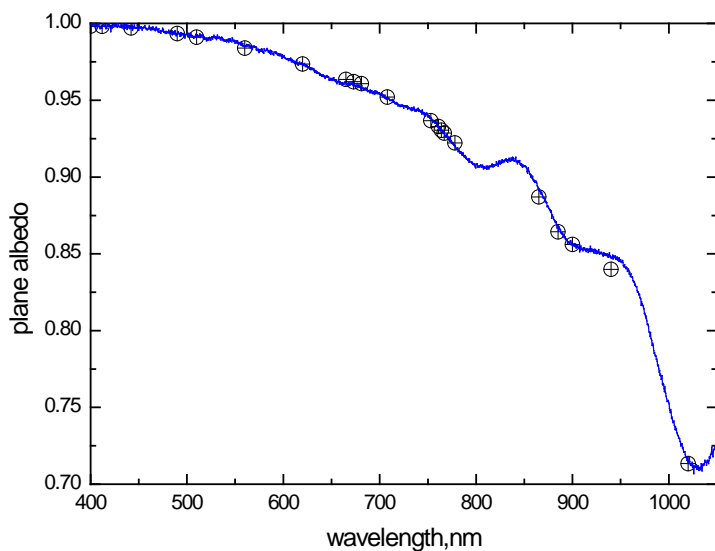


557  
558

559 Fig.2. The derived spectral probability of photon absorption for the case presented in Fig.1.

560

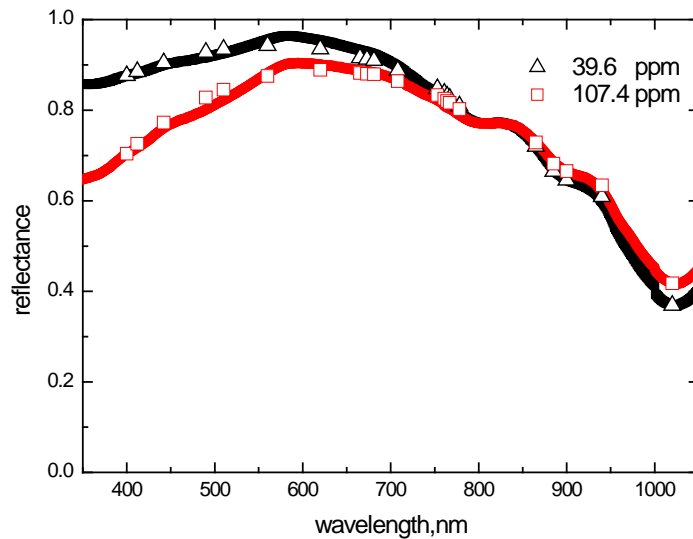
561



562  
563

564 Fig.3 The inter-comparison of theory (symbols) with experimental measurements of plane albedo  
565 (line) performed in Antarctica (Dome C, 75°5' S, 123°17' E) for pure snow. The measured plane  
566 albedo was obtained on 10/01/2017 at 23h24 UTC, for a solar zenith angle of 63 degrees. The  
567 parameters  $l$ ,  $f$ ,  $m$  have been derived from the measurements at 400, 560, and 1020nm.

568



570

571 Fig.4 The inter-comparison of theory (symbols) with experimental measurements (line) in  
 572 European Alps (45°55'56.70"N; 9°31'33.28" E) for the polluted snowpack. The parameters  $R_0$ ,  $l$ ,  
 573  $f$ ,  $m$  have been derived from the measurements at 400, 560, 865 and 1020nm.  
 574 Reflectance measurements were collected on snow containing different concentration of dust:  
 575 39.6 ppm (black line) and 107.4 ppm (red line). The dust has been collected from the upper snow  
 576 layer ( $\approx 5$ cm). Snow was clean at larger depths. A complete description of this dataset is  
 577 presented in Di Mauro et al. (2015).

578